Synthetic oligorotaxanes exert high forces when folding under mechanical load

Damien Sluysmans[1], Sandrine Hubert[1], Carson J. Bruns[2], Zhixue Zhu[2], J. Fraser Stoddart[2], Anne-Sophie Duwez[1]*

[1]UR MolSys, University of Liège, B6a Sart-Tilman, 4000 Liège, Belgium.

[2]Department of Chemistry, Northwestern University, Evanston, Illinois 60208-3113, USA.

*Correspondence to: asduwez@ulg.ac.be.

Combining the exquisite complexity of folded molecular architectures[1,2] and mechanically interlocked molecules[3-5], donor-acceptor oligorotaxane foldamers were recently synthesized[6]. So far, their mechanochemical properties, and thus their potential as pieces of advanced molecular machinery, are unknown. Here, using AFM-based single-molecule force spectroscopy, we mechanically unfolded oligorotaxanes, made of oligomeric dumbbells incorporating 1,5-dioxynaphthalene units encircled by cyclobis(paraquat-*p*-phenylene) rings. Real-time capture of fluctuations between unfolded and folded states reveals that the molecules exert forces of up to 50 pN against a mechanical load of up to 150 pN, and displays transition times of less than 10 μs. While the folding is as fast as that observed in proteins, it is remarkably more robust, thanks to the mechanically interlocked structure. Our results show that oligorotaxanes have the potential to exceed the performance of natural foldamers-based machines.

Folding is a ubiquitous process that nature uses to control the conformations of its molecular machines so as to perform chemical and mechanical tasks. Over the years, chemists have synthesized foldamers that adopt well-defined and stable folded architectures, mimicking the control expressed by natural systems in their three-dimensional arrangements[1,2]. Mechanically interlocked molecules, such as rotaxanes and catenanes, are prototypical molecular machines that enable the controlled movement and positioning of their component parts[3-5]. The mechanical bonds maintain precise co-conformations that confer upon molecules specific properties and functionality, such as movement, transport, and catalysis, to name but a few. The concept of simple [2]rotaxanes —a dumbbell encircled by a ring— has evolved in the past 10 years into more complex structures[3]. Recently, combining the exquisite complexity of these two classes of molecules, the syntheses of well-defined and function-designed compounds have emerged[6-10]. Among these, donor-acceptor oligorotaxane foldamers, in which interactions between the mechanically interlocked component parts dictate the single-molecule assembly of a folded secondary structure, have been proposed[6,8,9]. The unique folding motif is based on flexible poly(ethylene oxide) (PEO) dumbbells bearing 1,5-dioxynaphthalene (DNP) donors, which fold their way through a series of cyclobis(paraquat-*p*-phenylene) ($CBPQT^{4+}$) acceptor rings, also known as the little Blue Boxes[11], in a serpentine-like fashion in order to enable extended donor–acceptor (D–A) stacking interactions between the DNP units (red in Fig. 1) and the electron-poor 4,4'-bipyridinium ($BIPY^{2+}$) units in the $CBPQT^{4+}$ rings (blue in Fig. 1). The large number of π-stacks occurring between the donor and acceptor groups confers a compact folded secondary structure upon the molecule, as shown by X-ray crystallographic studies, ^{1}H NMR spectroscopy in solution, and computational modelling studies[6,8,9,12,13]. PF_6^- counterions also intercalate[12] in these folded (co)-conformations to neutralize the four positive charges on each ring and counteract the Coulomb repulsion, further stabilizing the structure. Molecular dynamics simulations have

shown that the folding is energetically favoured but entropically penalized, with the energetic contributions overcoming the entropy penalty and effectively driving the folding[13].

Much of the exquisite and detailed information on the structure, dynamics and operation of natural complex functional molecules and machines have been obtained from single-molecule force spectroscopy[14-19]. During these experiments, the molecule of interest is trapped and pulled between a substrate and a microscopic probe, and the restoring force is measured. AFM-based force spectroscopy is able to probe the mechanical properties of molecules with sub-nanometer resolution[14,16,17,20]. It has been widely used to elucidate the conformations of (bio)macromolecules[14], to study the mechanochemistry of biological machines[17], to understand the binding process between molecular partners[21,22], to investigate the mechanochemical processes in rotaxanes, catenanes and other mechanically interlocked compounds[23-25], etc.

Here, we describe how we have used AFM-based force spectroscopy to investigate the folding propensity of oligorotaxanes under mechanical load at the single-molecule level and provide information on their mechanochemical properties. The oligorotaxanes are terminated by bulky stoppers which prevent the rings from dethreading and 1,2-dithiolane rings at both their ends in order to allow strong interactions with the gold-coated substrate and tip. They were grafted in solution onto a gold-coated silicon surface, following our previously published strategy[24] to obtain a sparse distribution of the molecules on the surface (see Supplementary information) and optimize the interactions of single molecules with the tip. During the force spectroscopy measurements, a gold-coated silicon AFM tip approaches the oligorotaxane-functionalized substrate and strong Au-S interactions with the free end of the oligorotaxane are created. Then, increasing the distance between the tip and the surface, the behaviour of the molecule under extension is monitored by the deflection of the flexible tip-bearing cantilever (Fig. 2a).

Force-extensions profiles were obtained in *N*,*N*-dimethylformamide (DMF). A characteristic and reproducible sawtooth profile (Fig. 2b) with equally separated peaks was observed. Interestingly, the pattern is made of an alternation of higher and smaller peaks. We attribute this pattern to the sequential rupture of the intramolecular interactions between each $CBPQT^{4+}$ ring and the unoccupied DNP units on both of its sides. The alternation of higher and smaller peaks can be explained by the unfolding cooperativity: when an interaction is broken, the symmetrical one at the other side of the $CBPQT^{4+}$ ring is weakened and can be broken more easily. The mean rupture forces, between 100 and 150 pN (Fig. S3), are consistent with the breaking of weak noncovalent interactions like hydrogen bonds, electrostatic interactions, π-stacking and C–H–π interactions[26]. The last peak on the curves displays a higher force, of up to 300 pN, an observation that is characteristic of an S–S interaction with gold[27].

To support our hypothesis, we measured the length increments between successive rupture peaks (Fig. 2b) with the use of the worm-like chain (WLC) model[28], an entropic elasticity model that predicts the relationship between the extension of a flexible polymer and its entropic restoring force. Interestingly, the repetition of rupture peaks equally separated by a contour length increment (ΔL_c) of about 1.2 nm was observed, as depicted by the main population in the ΔL_c distribution (Fig. 2c). Considering the X-ray crystallographic data obtained for crystals grown from a solution of oligorotaxanes[6,9,12], it seems reasonable to attribute the ΔL_c of 1.2 nm to the breaking of the interaction linking one side of a $CBPQT^{4+}$ ring to the neighbouring DNP unit. Indeed, the theoretical distance between two subsequent DNP units in a locally folded conformation is about 0.7 nm, whereas this distance rises to almost 1.9 nm for the extended PEO segment in the locally unfolded conformation (see Supplementary information). Therefore, the expected difference in length between locally folded and unfolded states is 1.2 nm (Fig. 2a), which nicely matches the value measured here.

In less frequent cases, the disappearance of the small peaks (Fig. 2d) gives rise to higher contour length increments (ΔL_c centered at 2.3 nm, the second population in Fig. 2c), which can be attributed to the unfolding of two symmetrical repeating units almost simultaneously. This observation of missing peaks in force curves, and thus a ΔL_c twice (or more) as high, has already been observed by others in proteins containing repeating units separated by a few nanometers[29]. The role of unfolding cooperativity in such systems with repeating segments close to each other has been proposed to explain the populations of ΔL_c at double values. When an interaction is broken, the next one is weakened and can be broken easily and rapidly, causing a missing peak in the curves, and thus a doubling of ΔL_c. Here, the existing symmetry on both sides of the $CBPQT^{4+}$ ring, and the very short distance (~1 nm) involved, is consistent with a local cooperativity that makes the probability of nearly simultaneous breaking of the symmetrical interactions rather likely. On the basis of the highly defined ΔL_c populations observed in characteristic reproducible sawtooth patterns, we can also exclude the attribution of the multi-peak pattern to the detachment of multiple interactions (randomly distributed) of the molecule with the tip. The unfolding pattern is thus in good agreement with the previously proposed folded (co)-conformation in solution[6,8,9].

Pulling-relaxing experiments were then performed (Fig. 3). A single molecule was trapped between the tip and the substrate, and retraction-approach cycles were performed repeatedly. The force *versus* z-displacement curves show sequential breaking and reforming of a single interaction within the foldamer against the mechanical load. These four successive cycles performed on a single interaction demonstrate the reversibility of the unfolding and the robustness of the system. Moreover, rapid fluctuations between folded and unfolded states were detected, both in the pulling and relaxing curves (Figs. 3 and 4a). By inspecting the standard pulling curves at higher loading rates (Fig. S4), rapid transitions between two peaks were also observed. These quick fluctuations between two subsequent unfolding peaks

provide evidence for the thermodynamic equilibrium between locally folded and unfolded states when the molecule is under an external load. Very few examples of observing fluctuations in real time have been described in the literature. Fluctuations were observed for the first time in RNA molecules under an external load applied with optical tweezers[30]. The RNA molecules were shown to fluctuate back and forth between two conformations when the loading rate was small enough to approach thermal equilibrium conditions or when kept under a constant low force. These fluctuations can be explained by the reforming of an interaction a short time after being broken. This phenomenon, called *hopping*, has also been observed[31] in RNase H. Later, real-time binding-unbinding transitions of calmodulin[32,33] and reversible unfolding-refolding of an α/β protein[34] were observed by AFM-based force spectroscopy. Here, we observe, for the first time we believe, such fluctuations in a significantly smaller synthetic molecule and at much higher velocities. The distributions of the external load (F_{app}) applied to the locally unfolded oligorotaxane and the force exerted (ΔF) by the molecule to regain its locally folded state are shown in Fig. 4b and 4c, respectively. These distributions show that the molecule is able to exert a force (ΔF) of 25 pN on average, up to 50 pN, against an external load (F_{app}) of 60 pN, to refold and remake the broken interactions during the pulling experiment. In an attempt to obtain more details on the kinetics of these fluctuations, we focused (Fig. 4d) on the force *versus* time curves during the hopping events. At the highest loading rate (10^5 pN·s^{-1}), we measured a fluctuation rate of more than 4300 per second (Fig. S5). If we compare to the fluctuation rate measured for natural folding proteins like calmodulin[33], it is more than 300 times higher. One fluctuation between partially unfolded and folded states happens in less than 10 µs, which makes the oligorotaxane the fastest folding system ever measured at such high loading rates.

As these transitions can, in principle, be observed near the equilibrium, i.e., when the speed of the experiment is lower than the binding-unbinding kinetics, we can compare

qualitatively the results for the synthetic oligorotaxanes with those obtained previously for folding proteins under the same conditions. Since we have observed the hopping phenomenon on the full range of loading rates —10^3 to 10^5 pN·s^{-1}, which is 100 to 1000 times higher than those previously tested for natural folding proteins[30-34]—, we can conclude with good reason that the folding motifs made of mechanically interlocked components are much more robust than the classical ones in the proteins investigated previously by AFM or by employing optical tweezers. The robustness also manifests itself in the intensity of the mechanical load against which the molecule can refold. The maximum mechanical load that folding proteins can accommodate when fluctuating between unfolded and folded states during the pulling experiment is typically in the order of 10 pN[30-34]. Although several proteins are able to refold during relaxing experiments, when the tension exerted by the probe is released, the refolding during the pulling regime is a much rarer event and, in the few examples described in the literature, the mechanical load was limited to 10 pN. Here, the oligorotaxane can refold during the force increasing regime against a load of 60 pN on the average, up to 150 pN. This remarkably robust behaviour can be explained by the mechanically interlocked components which restrict the degrees of freedom and stay in close proximity after the interaction breaks. The mechanically interlocked structure constrains the rings around the DNP recognition sites and favours a defined geometry that pre-orient the partners, decreasing the degrees of freedom and thus facilitating the refolding. The proximity ensures that the entropic penalty is low. It is thus possible, even under a high external load, to counteract the small increase of entropy and reform the interactions rapidly. Larger natural biological folds rely upon weak interactions amongst a significant number of constituents, all covalently bound in a single molecule. These folding interactions are opposed by the folding entropy which roughly scales as the number of constituents involved in the fold. When a load is applied, a cascade of disrupted interactions occurs, driven by a high gain in entropy. Compared to biological counterparts, the

refolding of oligorotaxanes is associated with a low entropy decrease that can be opposed by the enthalpic gain on account of the strong electron donor-acceptor interactions. The entropy drive to distort the fold is not so great, as the fold consists of only four ethylene oxide units and four C–C/C–O bonds. The fold in the oligorotaxanes can thus sustain a large load. The entropy plays a greater role in the unfolding of a protein, lowering the force against which the fold can be sustained.

Our results show that donor-acceptor oligorotaxanes, wherein the dumbbells are composed of oligoether chains interrupted by 1,5-dioxynaphthalene units, half of which are encircled by cyclobis(paraquat-*p*-phenylene) rings[6], are able to exert significant forces in refolding against a high external load. The observation of fluctuations, even at high loading rates, implies that the thermal dynamics of these molecules are very high, making them the fastest ever measured at such high loading rates. The mechanically interlocked structure of the oligorotaxanes is most likely responsible for this remarkably robust and highly dynamic folding. Taking inspiration from nature's molecular machinery that makes use of well-defined, stable, but highly dynamic systems, the emerging class of synthetic oligorotaxane foldamers reported here reveal themselves to be efficient, robust and intricately regulated by their dynamics. Our results show that oligorotaxanes have the potential to exceed the performance of natural foldamers.

Methods

Oligorotaxane synthesis. The [5]rotaxanes were synthesized according to a protocol described recently[6]. Briefly, this one-pot synthesis uses a copper-catalyzed azide-alkyne cycloaddition to thioctic ester-functionalized stoppers at both ends of the DNP-derived polyether chains in the presence of $CBPQT^{4+}$ rings. Using conventional chromatographic

techniques, oligorotaxanes with half the DNP units encircled by a ring were isolated. The molecules were characterized by NMR spectroscopy and mass spectrometry[6].

Immobilization of the oligorotaxanes molecules on surfaces. The oligorotaxanes were grafted onto gold-coated silicon substrates using our previously established method[24] to obtain a sparse regime of the molecule of interest. The substrates were dipped for 1 h in a solution of the oligorotaxane (2 10^{-8}mol) containing 90 mol% of dodecyl disulfide in Me_2CO at room temperature. The role of the dodecyl disulfide is to ensure a dilute distribution of the oligorotaxanes on the surface and passivate the substrate. All the details are given in SI.

Single-molecule force spectroscopy experiments. Experiments were carried out with a PicoPlus 5500 microscope (Agilent Technologies) equipped with a closed-loop scanner. Gold-coated tips (OBL-10 Biolever, Bruker; nominal spring constant k=0.009–0.1 $N \cdot m^{-1}$) were used for all the force experiments. The spring constant of each cantilever was calibrated by the thermal noise and Sader methods.[35,36] The molecules were picked up for force experiments by gently pressing the AFM tip against the substrate. Force measurements were performed at loading rates between 10^3 and 10^5 $pN \cdot s^{-1}$. Pulling–relaxing cycles were realized using a custom-made routine to guide the tip. Each force curve contains 20,000 data points. All the details are given in SI.

References

1. Guichard, G. & Huc, I. Synthetic foldamers. *Chem. Commun.* **47,** 5933–5941 (2011).
2. Le Bailly, B. A. F. & Clayden, J. Dynamic foldamer chemistry. *Chem. Commun.* **52,** 4852-4863 (2016).

3. Bruns, C. & Stoddart, J. F. The Nature of The Mechanical Bond: From Molecules to Machines, Wiley, 2017.
4. Erbas-Cakmak, S., Leigh, D. A., McTernan, C. T. & Nussbaumer, A. L. Artificial molecular machines. *Chem. Rev.* **115**, 10081-10206 (2015).
5. Kay, E. R. & Leigh, D. A. Rise of the molecular machines. *Angew. Chem. Int. Ed.* **54**, 10080–10088 (2015).
6. Zhu, Z., Bruns, C. J., Li, H., Lei, J., Ke, C., Liu, Z., Shafaie, S., Colquhoun, H. M. & Stoddart, J. F. Synthesis and solution-state dynamics of donor–acceptor oligorotaxane foldamers. *Chem. Sci.* **4**, 1470-1483 (2013).
7. Zhang, K. D., Zhao, X., Wang, G.-T., Liu, Y., Zhang, Y., Lu, H.-J., Jiang, X.-K. & Li, Z.-T. Foldamer-tuned switching kinetics and metastability of [2]rotaxanes. *Angew. Chem. Int. Ed.* **50**, 9866–9870 (2011).
8. Bruns, C. J. & Stoddart, J. F. Mechanically interlaced and interlocked donor-acceptor foldamers. *Adv. Polym. Sci.* **261**, 271–294 (2013).
9. Basu, S., Coskun, A., Friedman, D. C., Olson, M. A., Benítez, D., Tkatchouk, E., Barin, G., Yang, J., Farhenbach, A. C., Goddard III, W. A. & Stoddart, J. F. Donor-acceptor oligorotaxanes made to order. *Chem. A Eur. J.* **17**, 2107–2119 (2011).
10. Wang, W.-K., Xu, Z.-Y., Zhang, Y.-C., Wang, H., Zhang, D.-W., Liu, Y. & Li, Z.-T. A tristable [2]rotaxane that is doubly gated by foldamer and azobenzene kinetic barriers. *Chem. Commun.* **52**, 7490–7493 (2016).
11. Odell, B., Reddington, M., Slawin, A., Spencer, N., Stoddart, J. F., & Williams, D. Cyclobis(paraquat-*p*-phenylene). A tetracationic multipurpose receptor. *Angew. Chem. Int. Ed.* **27**, 1547-1550 (1988).

12. Zhu, Z., Li, H., Liu, Z., Lei, J., Zhang, H., Botros, Y. Y., Stern, C. L., Sarjeant, A. A., Stoddart, J. F. & Colquhoun, H. M. Oligomeric pseudorotaxanes adopting infinite-chain lattice superstructures. *Angew. Chem. Int. Ed.* **51**, 7231–7235 (2012).
13. Franco, I., Schatz, G. C. & Ratner, M. A. Single-molecule pulling and the folding of donor-acceptor oligorotaxanes: phenomenology and interpretation. *J. Chem. Phys.* **131**, 124902—1-13 (2009).
14. Fisher, T. E., Marszalek, P. E. & Fernandez, J. M. Stretching single molecules into novel conformations using the atomic force microscope. *Nat. Struct. Biol.* **7**, 719–724 (2000).
15. Bustamante, C., Chemla, Y. R., Forde, N. R. & Izhaky, D. Mechanical processes in biochemistry. *Annu. Rev. Biochem.* **73**, 705–748 (2004).
16. Neuman, K. C. & Nagy, A. Single-molecule force spectroscopy: optical tweezers, magnetic tweezers and atomic force microscopy. *Nat. Methods* **5**, 491–505 (2008).
17. Puchner, E. M. & Gaub, H. E. Force and function: probing proteins with AFM-based force spectroscopy. *Curr. Opin. Struct. Biol.* **19**, 605–614 (2009).
18. Liang, J. & Fernandez, J. M. Mechanochemistry: one bond at a time. *ACS Nano* **3**, 1628–1645 (2009).
19. de Souza, N. Pulling on single molecules. *Nat. Methods* **9**, 873–877 (2012).
20. Molecular Manipulation With Atomic Force Microscopy, ed. A.-S. Duwez, N. Willet, CRC Press, Boca Raton, 2012.
21. Hinterdorfer, P. & Dufrene, Y. F. Detection and localization of single molecular recognition events using atomic force microscopy. *Nat. Methods* **3**, 347–355 (2006).
22. Müller, D. J. & Dufrêne, Y. F. Atomic force microscopy as a multifunctional molecular toolbox in nanobiotechnology. *Nat. Nanotechnol.* **3**, 261–269 (2008).
23. Janke, M., Rudzevich, Y., Molokanova, O., Metzroth, T., Mey, I., Diezemann, G., Marszalek, P. E., Gauss, J., Bohmer, V. & Janshoff, A. Mechanically interlocked

calix[4]arene dimers display reversible bond breakage under force. *Nat. Nanotechnol.* **4**, 225–229 (2009).

24. Lussis, P., Svaldo-Lanero, T., Bertocco, A., Fustin, C.-A., Leigh, D. A. & Duwez, A.-S. A single synthetic small molecule that generates force against a load. *Nat. Nanotechnol.* **6**, 553–557 (2011).
25. Van Quaethem, A., Lussis, P., Leigh, D. A., Duwez, A.-S. & Fustin, C.-A. Probing the mobility of catenane rings in single molecules. *Chem. Sci.* **5**, 1449–1452 (2014).
26. Hunter, C. A. Quantifying intermolecular interactions: Guidelines for the molecular recognition toolbox. *Angew. Chem. Int. Ed.* **43**, 5310–5324 (2004).
27. Beyer, M. K. & Clausen-Schaumann, H. Mechanochemistry: The mechanical activation of covalent bonds. *Chem. Rev.* **105**, 2921–2948 (2005).
28. Flory, P. J. Statistical mechanics of chain molecules. *Br. Polym. J.* **2,** 302–303 (1989).
29. Lee, G., Abdi, K., Jiang, Y., Michaely, P., Bennett, V. & Marszalek, P. E. Nanospring behaviour of ankyrin repeats. *Nature* **440**, 246-249 (2006).
30. Liphardt, J., Onoa, B., Smith, S. B., Tinoco, I. & Bustamante, C. Reversible unfolding of single RNA molecules by mechanical force. *Science* **292**, 733–737 (2001).
31. Cecconi, C., Shank, E., Bustamante, C. & Marqusee, S. Direct observation of the three-state folding of a single protein molecule. *Science* **309**, 2057-2060 (2005).
32. Junker, J. P. & Rief, M. Single-molecule force spectroscopy distinguishes target binding modes of calmodulin. *Proc. Natl. Acad. Sci. USA* **106**, 14361–14366 (2009).
33. Junker, J. P., Ziegler, F. & Rief, M. Ligand-dependent equilibrium fluctuations of single calmodulin molecules. *Science* **323**, 633–637 (2009).
34. He, C., Hu, C., Hu, X., Hu, X., Xiao, A., Perkins, T. T. & Li, H. Direct observation of the reversible two-state unfolding and refolding of an α/β protein by single-molecule atomic force microscopy. *Angew. Chem. Int. Ed.* **54**, 9921–9925 (2015).

35. te Riet, J., Katan, A. J., Rankl, C., Stahl, S. W., van Buul, A. M., Phang, I. Y., Gomez-Casado, A., Schon, P. , Gerritsen, J. W. , Cambi, A. , Rowan, A. E., Vancso, G. J. , Jonkheijm, P., Huskens, J., Oosterkamp, T. H., Gaub, H., Hinterdorfer, P., Figdor, C. G. & Speller, S. Interlaboratory round robin on cantilever calibration for AFM force spectroscopy. *Ultramicroscopy* **111**, 1659-1669 (2011)

36. Sader, J. E., Sanelli, J. A., Adamson, B. D., Monty, J. P., Wei, X., Crawford, S. A., Friend, J. R., Marusic, I., Mulvaney, P. & Bieske, E. J. Spring constant calibration of atomic force microscope cantilevers of arbitrary shape. *Rev. Sci. Instrum.* **83**, 103705, 1–16 (2012)

Acknowledgements

D. S. thanks the Fonds de la Recherche Scientifique-Fonds National pour la Recherche Scientifique (FRS-FNRS) for his FRIA fellowship. The research was supported by the project PDR T.0205.13 of the FRS-FNRS at University of Liège and by the King Abdulaziz City of Science and Technology (KACST) as part of their Joint Center of Excellence in Integrated Nano-Systems (JCIN) at Northwestern University.

Author contributions

D. S. and S. H. performed the AFM experiments and analysed the data. C. B. and Z. Z. carried out the oligorotaxane synthesis and characterization studies. A-S.D. and J.F.S. designed the experiments. A-S. D. and D. S. prepared the manuscript. All the authors discussed the data and commented on the manuscript.

Additional information

Supplementary information is available on the online version of the paper. Reprints and permission information is available online at http://www.nature.com/reprints. Correspondence and requests for materials should be addressed to A.-S.D.

Competing financial interests

312 The authors declare no competing financial interests.

313

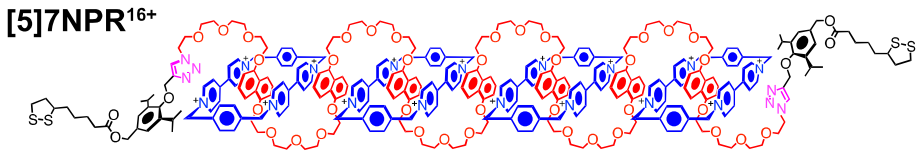

Figure 1. **Structure formula and co-conformation of the [5]oligorotaxane ([5]7NPR^{16+}) of the [0.5(*n*–1)+2] family**. The terms in square brackets denote the total number of interlocked components and *n* is the number of DNP units in the dumbbell.[6] In this co-conformation, half of the dioxynaphthalene (DNP) units (in red) are encircled by cyclobis(paraquat-*p*-phenylene) (CBPQT^{4+}) rings (in blue). The serpentine-like folding arises from π-stacks between DNP units and bipyridinium charged rings, hydrogen bonds linking alpha-hydrogen atoms of the rings with poly(ethylene oxide) of the dumbbells, and Coulombic interactions between the PF_6^- counterions and the rings. PF_6^- counterions are not shown.

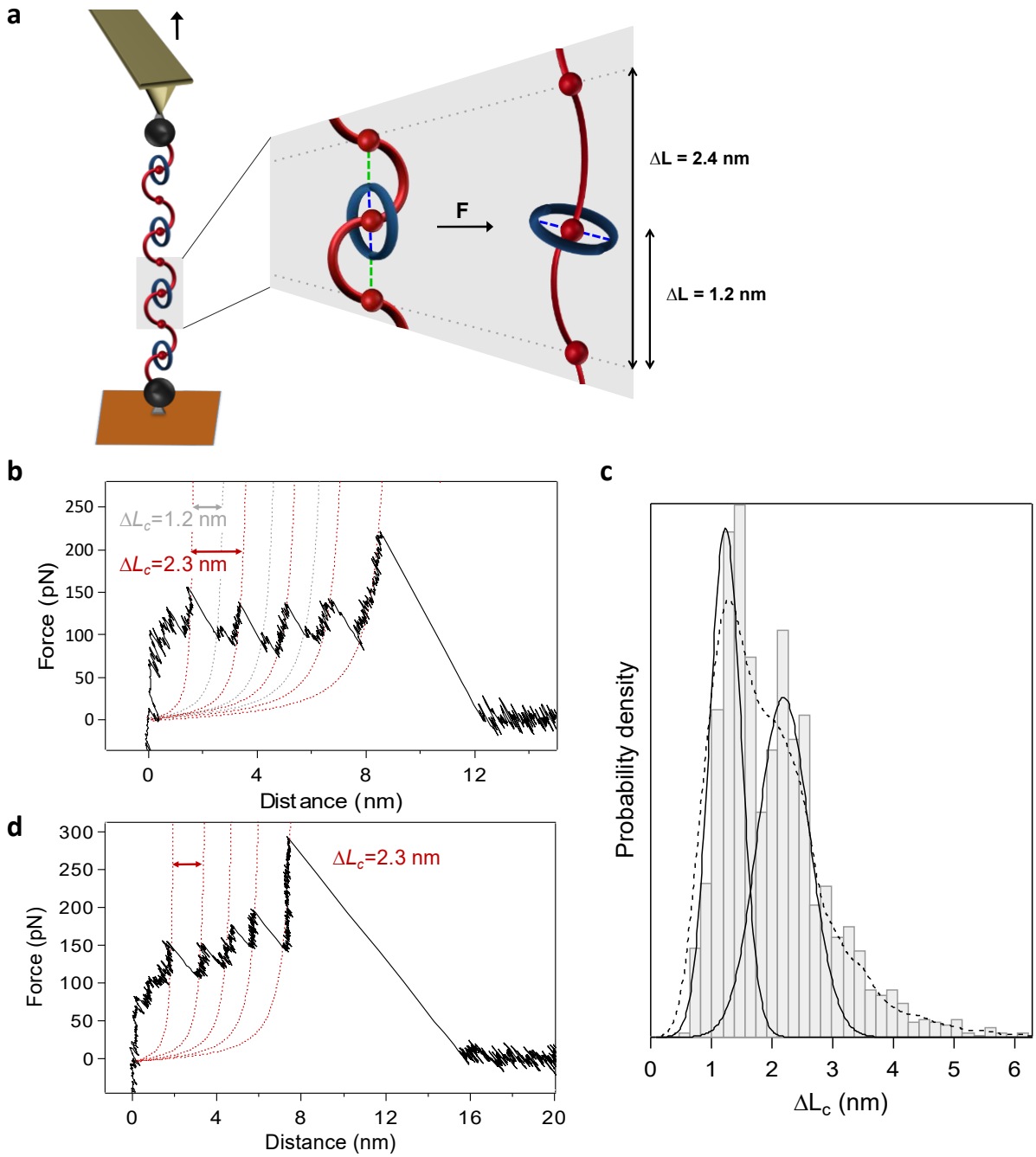

Figure 2. AFM-Based mechanical unfolding of the [5]oligorotaxane in DMF. a. Illustration of the pulling experiment. Mechanical unfolding occurs by retracting the cantilever at a constant velocity. The theoretical variation of length after the breaking of one interaction between a free DNP and the contiguous ring is about 1.2 nm, on the basis of crystallographic data (see the details in SI). **b**. Example of a force-distance curve obtained at 40 nm·s^{-1} (10^3 pN·s^{-1}) showing a characteristic reproducible saw-tooth profile. Each peak is fitted with the WLC model to obtain contour length increments (ΔL_c) values. **c**. Distribution

of the contour lengths increments (ΔL_c) between successive peaks ($N = 1712$). Histograms, Gaussian mixture model (GMM) multiple populations, and probability density function (PDF) are shown. **d**. Example of a force-distance curve obtained at 350 nm·s^{-1} (10^4 pN·s^{-1}) showing a characteristic reproducible saw-tooth profile with missing every second peak.

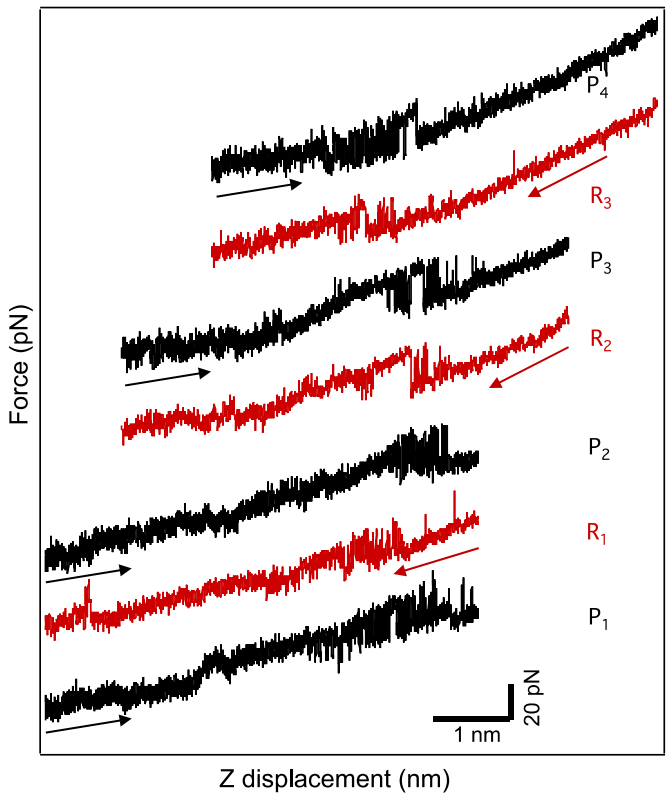

Figure 3. Pulling-relaxing cycles showing the reformation of one interaction under mechanical load. Pulling(P)-relaxing(R) curves (down-top) showing sequential folding and unfolding of a single interaction in an individual [5]oligorotaxane molecule in DMF. Hopping from one co-conformation to the other is observable during pulling and relaxing. (Pulling at 10 nm·s^{-1} (300 pN·s^{-1}) and relaxing at 4 nm·s^{-1} (120 pN·s^{-1})).

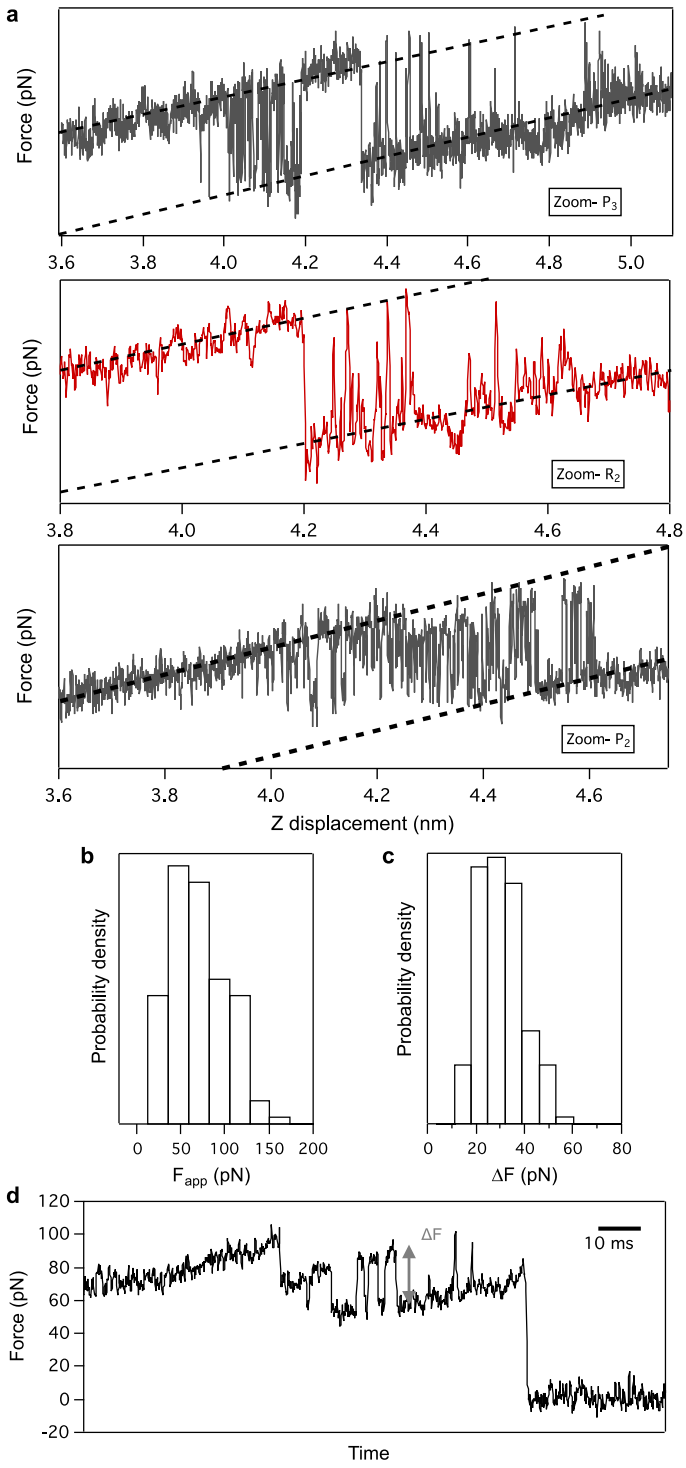

Figure 4. **Pulling-relaxing experiments showing the numerous fluctuations between folded and unfolded states during the breaking and reformation of one interaction.** **a.** Pulling-relaxing cycles obtained on an individual [5]oligorotaxane molecule in DMF. The figures are magnifications of the force curves shown in Fig. 3 (P3, R2 and P2). **b.** Distribution of the external force applied before the fluctuations from locally unfolded to locally folded

states (N = 115). The histogram shows the maximum external force against which the oligorotaxane is able to refold. **c.** Distribution of the force increment during fluctuations (N = 115). During the local folding, the oligorotaxane exerts a force of 25 pN on the average, up to 50 pN (loading rate of 10^4 pN·s^{-1}). **d.** Force-time curve (loading rate of 10^4 pN·s^{-1} (350 nm·s^{-1})).